X-ray Crystal Structures of Staphylococcal Nuclease Complexed with the Competitive Inhibitor Cobalt(II) and Nucleotide[†,‡]

Patrick J. Loll,[*,§] Stephen Quirk,[∥,⊥] Eaton E. Lattman,[∥] and R. Michael Garavito[§]

Department of Biochemistry and Molecular Biology, University of Chicago, 920 East 58th Street, Chicago, Illinois 60637, and Department of Biophysics and Biophysical Chemistry, Johns Hopkins University School of Medicine, 725 North Wolfe Street, Baltimore, Maryland 21205

Received October 28, 1994; Revised Manuscript Received January 25, 1995[⊗]

ABSTRACT: Two crystal structures of ternary complexes of staphylococcal nuclease, cobalt(II), and the mononucleotide pdTp are reported. The first has been refined at 1.7 Å to a crystallographic *R* value of 0.198; the second, determined from a crystal soaked for 9 months in a slightly different mother liquor than the first crystal, has been refined at 1.85 Å to an *R* value of 0.174. In the first structure, the cobalt ion is displaced 1.94 Å from the normal calcium position, and the active site is dominated by a salt bridge between Asp-21 and Lys-70* from a symmetry-related molecule in the crystal lattice. The Co^{2+} ion appears unable to displace this lysine; consequently, the metal is bound in a vestibular site adjacent to the calcium site. The metal-binding pocket in the second structure adopts a configuration similar to that of the calcium complex, with the cobalt ion binding only 0.36 Å from the calcium position. However, an inner sphere water seen in the calcium structure is missing from this structure. The cobalt ion in the second structure appears to be loosely or transiently coordinated within the calcium binding pocket, as evidenced by the high value of its refined thermal factor. Loss of catalytic activity for cobalt(II)-substituted nuclease is perhaps due to its inability to bind this inner sphere water.

Staphylococcal nuclease (SNase,[1] EC 3.1.4.4) is a Ca^{2+}-dependent extracellular phosphodiesterase that cleaves a variety of nucleic acids to 3′-phosphomono- and dinucleotides. It has been extensively studied biochemically [for example, see Cotton *et al.* (1979), Tucker *et al.* (1979), Sondek and Shortle (1990), and Hale *et al.* (1993)], crystallographically (Arnone, 1971; Cotton *et al.*, 1979; Loll & Lattman, 1989; Hynes & Fox, 1991), and by NMR methods (Torchia *et al.*, 1989; Stanczyk & Bolton, 1992; Evans *et al.*, 1989; Loh & Markley, 1994). SNase accelerates the cleavage of phosphodiester bonds by a factor of 10^{16} and has been suggested to be one of the most proficient enzymes studied (Radzicka & Wolfenden, 1995); hence, given the wealth of structural and biochemical information available about the enzyme, it affords an excellent model for the investigation of the structural bases underlying enzymatic catalysis.

Most mechanisms that have been proposed for the SNase-mediated cleavage of phosphodiester bonds are predicated upon general base catalysis carried out by Glu-43. The models postulate that Glu-43 activates a water molecule bound in the active site which, in turn, attacks the phosphodiester bond (which has been at least partially charge-neutralized by positively charged moieties in the active site), forming a trigonal bipyramid transition state. After loss of the 5′-hydroxyribose leaving group, the transition state collapses with inversion of configuration at the phosphate (Mehdi & Gerlt, 1982). Unfortunately, site-directed mutagenesis experiments intended to elucidate the catalytic role of Glu-43 have been complicated by concomitant structural changes in the enzyme (Hibler *et al.*, 1987; Wilde *et al.*, 1988; Loll & Lattman, 1990). In addition, recent results (Judice *et al.*, 1993; Hale *et al.*, 1993) have cast doubt on the importance of any general base contribution from Glu-43, thereby raising the question of whether the essential calcium ion performs the function hitherto assigned Glu-43.

Calcium is required for SNase activity; while other metal ions bind to the enzyme, none can activate it fully, and most support no activity at all (Tucker *et al.*, 1978). In particular, Co^{2+} is a linear competitive inhibitor with respect to Ca^{2+}, but the SNase−Co^{2+} complex does not catalyze the hydrolysis of DNA or RNA at measurable levels (Mildvan & Serpersu, 1989). The paramagnetic nature of Co^{2+} has enabled its extensive use as an active site probe of SNase (Serpersu *et al.*, 1986, 1988). The competitive nature of Co^{2+} binding has given researchers confidence that Co^{2+} occupies the calcium site and that Co^{2+}-substituted nuclease represents a reasonable structural model for the active enzyme. Hence, information derived from solution studies of the Co^{2+}-substituted enzyme has been used to determine the conformations of the enzyme-bound substrate dTdA (Weber *et al.*, 1991) and the enzyme-bound inhibitor pdTp (Weber *et al.*, 1993), allowing these compounds to be docked into the

[†] Supported by Damon Runyon−Walter Winchell Cancer Research Fund fellowship 1054 (P.J.L.), NRSA GM15959-01 (S.Q.), NIH GM36358 (E.E.L.), and PHS/NIH shared instrumentation Grant RR06568 (RMG).

[‡] The final refined coordinates of all structures presented herein have been deposited in the Protein Data Bank (entry names 1STG and 1STH).

* Corresponding author. Telephone: (312) 702-0286. Fax: (312) 702-0439. E-mail: loll@biovax.uchicago.edu.

[§] University of Chicago.

[∥] Johns Hopkins University School of Medicine.

[⊥] Present address: School of Chemistry and Biochemistry, Georgia Institute of Technology, Atlanta, GA 30332.

[⊗] Abstract published in *Advance ACS Abstracts,* March 15, 1995.

[1] Abbreviations: SNase, staphylococcal nuclease; pdTp, thymidine 3′,5′-bisphosphate; MPD, 2-methyl-2,4-pentanediol; rms, root mean square; Co1, SNase−Co^{2+}-pdTp model number 1, corresponding to PDB entry 1STG; Co2, SNase−Co^{2+}-pdTp model number 2, corresponding to PDB entry 1STH.

0006-2960/95/0434-4316$09.00/0

crystallographic model of the enzyme's active site (Weber *et al.*, 1992) and allowing for a structurally detailed mechanistic proposal that combines X-ray and NMR results.

We have determined the X-ray crystal structures of two SNase−Co^{2+}−pdTp complexes in an effort to understand the role of the metal ion in catalysis and to provide an independent test of the validity of mechanistic proposals based on the structure of the SNase−Co^{2+} complex. While identical in composition, these complexes have different structures in the vicinity of the metal-binding site. In this paper we describe these crystal structures, compare them with each other and with the SNase−Ca^{2+}−pdTp structure, and draw inferences from them about the nature of metal binding by SNase and possible roles for the essential calcium ion.

MATERIALS AND METHODS

Protein Isolation and Crystallization. Purified wild-type SNase was a gift from A. Meeker and D. Shortle (Johns Hopkins University School of Medicine, Baltimore). Crystals of the protein, in a complex with Co^{2+} and the inhibitor thymidine 3′,5′-bisphosphate (pdTp), were grown from 2-methyl 2,4-pentanediol (MPD) at 4 °C essentially as described (Loll & Lattman, 1989), substituting $CoCl_2$ for $CaCl_2$. The crystals grew to full size within several weeks, after which they were harvested and transferred to a stabilization buffer (40% MPD in 30 mM Tris-Cl, pH 8.15, 50 μM $CoCl_2$, 100 μM potassium citrate, and 50 μM pdTp) and maintained in a depression plate in a sealed sandwich box at 4 °C . After 1 week one crystal was selected and used to collect data set 1. A second crystal was removed 9 months later and used to collect data set 2. At this time it was evident that water had evaporated from the sandwich box and that the MPD concentration was significantly higher than 40%, although no attempt was made to measure the actual concentration.

Data Collection. Diffraction data sets 1 and 2 for the SNase−Co^{2+}−pdTp complex were collected with the Enraf-Nonius FAST (Fast scanning Area Sensitive TV detector) area detector. Each data set was taken from a single crystal maintained at 4 °C. Both data sets were assembled from eight separate scans. The individual data scans were integrated and profile-fit using the MADNES and PROCOR software packages (Messerschmidt & Pflugrath, 1987; Kabsch, 1988) and were combined and scaled by the PROTEIN package (Steigemann, 1974). For data set 1, the crystal's c^* axis was aligned with the rotation axis so as to optimize measurement of the anomalous signal from the cobalt ion. Data set 2 was collected in a random orientation. Data collection statistics are summarized in Table 1.

Structure Solution and Refinement. Both cobalt complex crystals are isomorphous with crystals of the wild-type staphylococcal nuclease−Ca^{2+}−pdTp complex (Loll & Lattman, 1989; PDB entry 1SNC), and so this latter structure was used as the initial model for both refinements.

Refinement of Data Set 1. A native anomalous difference Patterson map calculated using data set 1 suggested that the cobalt ion occupied a different position than the calcium ion in the SNase−Ca^{2+}−pdTp complex; this observation was confirmed by a cobalt − calcium difference Fourier map which showed a single large negative peak centered on the calcium position and a single large positive peak roughly 2 Å away (see Figure 1). Accordingly, the metal ion and pdTp molecule were omitted from the initial refinement steps. The initial crystallographic R value for the model containing residues 7−141 of the protein was 0.34 for all 6−2.0 Å data having F greater than 2 times $\sigma(F)$. Using the program X-PLOR (Brunger, 1992), this model was subjected to rigid body refinement, simulated annealing, individual B value refinement, and refinement of the overall anisotropic ΔB values, which reduced the R value to 0.24. Calculation of $F_{obs} - F_{calc}$ and $2F_{obs} - F_{calc}$ maps at this stage clearly revealed the positions of the cobalt ion and the nucleotide, confirming our initial suspicion that the cobalt ion occupies a different position than the calcium position. The metal ion and nucleotide were built into the map, and refinement was continued in an iterative manner, with cycles of positional and B value refinement in X-PLOR alternating with cycles of rebuilding and placement of water molecules. In the final stages of the refinement, alternate conformations were included for four protein side chains, none of which are close to the metal-binding site. The refinement of model 1 was judged to have converged after 51 water molecules had been added; at this point, the highest and lowest values seen in the $F_{obs} - F_{calc}$ map were 0.18 and −0.16 electrons/Å^3, respectively. Details of this refinement are given in Table 1. This model will be referred to as Co1.

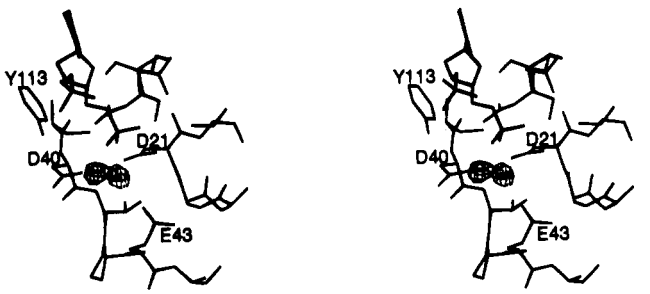

FIGURE 1: Stereoview of the $F_{obs\ cobalt} - F_{obs\ calcium}$ difference Fourier map, computed with phases calculated from the SNase−Ca^{2+}−pdTp structure and superimposed upon a model of the calcium complex structure. Two contour levels are shown: The dotted lines represent a contour level of -9σ (where σ equals the standard deviation of the map) while the solid lines represent a level of $+8\sigma$. The position of the calcium ion is shown by the cross lying directly under the negative peak. The positive peak is centered at a point roughly 2 Å away.

Refinement of Data Set 2. The large difference in unit cell constants between data sets 1 and 2 suggested that the two structures might not be the same. The native anomalous difference Fourier and the cobalt − calcium difference Fourier maps confirmed this, indicating that the cobalt ion in structure 2 is close to the position occupied by the calcium ion in the SNase−Ca^{2+}−pdTp complex. For this reason, the initial model included inhibitor and metal as well as amino acids 7−141. Apart from this difference, the refinement followed essentially the same strategy as the refinement of model 1 described above. The R value was reduced from an initial value of 0.38 to 0.21 after performing rigid body refinement, simulated annealing, positional and thermal factor refinement using conventional conjugate gradient minimization, refinement of an overall anisotropic ΔB, and small manual adjustments of the model. Next, omit $F_{obs} - F_{calc}$ electron density maps were calculated to examine the active site region around the metal ion. The cobalt ion and a sphere of 4 Å surrounding the metal were omitted from a map calculation, refit to density, and then refined. Water molecules were added to the model at this time. Rebuilding,

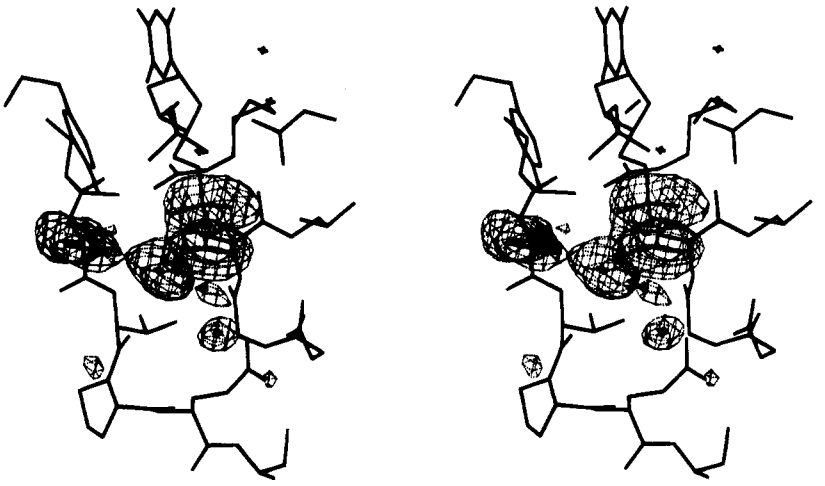

FIGURE 2: Stereoview of an omit electron density map showing the active site of the Co1 structure. The map was computed with coefficients of the form $F_{obs} - F_{calc}$, where F_{calc} was calculated from a model from which the metal ion and its ligands were omitted. The map is contoured at the 3σ level.

Table 1: Data Collection and Refinement Statistics for SNase−Co^{2+}-pdTp Complexes

	Co1	Co2
space group	$P4_1$	$P4_1$
unit cell dimensions (Å)		
a, *b*	48.21	47.48
c	63.26	63.21
data collection statistics		
resolution (Å)	6.0−1.70	6.0−1.85
no. obs	22 450	87 667
no. unique	11 897	11 570
R_{merge}	0.035	0.048
completeness (%)	74	99
final refinement parameters		
no. of non-hydrogen atoms	1169	1176
no. of water molecules	51	58
resolution (Å)	6.0−1.70	6.0−1.85
final *R* value	0.198 (all data)	0.174 (all data)
rms deviation from ideal geometry of final model		
bond lengths (Å)	0.016	0.014
bond angles (deg)	3.07	2.99
dihedral angles (deg)	25.2	25.1
improper angles (deg)	1.31	1.16

solvent fitting, and refinement were continued in an iterative manner until convergence was achieved, giving the final model 2. The *R* value for this model for all observed structure factors between 6.0 and 1.85 Å is 0.174; the maximum and minimum values of the $F_{obs} - F_{calc}$ map calculated at this point are 0.27 and −0.24 electrons/Å^3, respectively. Details of the refinement are given in Table 1. This model will be referred to as Co2.

RESULTS

Quality of the Models. Refinement statistics for both SNase−Co^{2+}−pdTp structures are shown in Table 1. Both models consist of residues 6−141, one Co^{2+} ion, and one pdTp molecule; model 1 includes 51 water molecules and 4 alternate side chain conformations, while model 2 includes 58 water molecules. Both structures have been refined at high resolution to low *R* values and are comparable in quality to the SNase−Ca^{2+}−pdTp structure. The models exhibit excellent geometry, with all ϕ/ψ angle pairs falling within allowed regions of Ramachandran space, except for those of Asn-138. This residue, however, adopts similar conformations in the SNase−Ca^{2+}−pdTp and apo-SNase structures (Loll & Lattman, 1989; Hynes & Fox, 1991). Luzatti analysis (data not shown) yields estimates for the mean coordinate errors for Co1 and Co2 of 0.25 and 0.20 Å, respectively.

Positions of the cobalt ion and amino acid residues in the vicinity of the metal binding pocket of both structures were particularly carefully modeled. Extensive use of omit $2F_{obs} - F_{calc}$ and omit $F_{obs} - F_{calc}$ electron density maps was made to confirm the positions of the cobalt ion and of its ligands. In both structures, this entire region is well defined in both the $2F_{obs} - F_{calc}$ and the omit $F_{obs} - F_{calc}$ electron density maps, indicating a robust modeling of the entire region (e.g., see Figures 2 and 3). The final refined positions of the metal ions in both structures are in good agreement with the positions predicted by strong peaks in the native anomalous difference Fourier syntheses computed with calculated phases derived from the calcium structure. In addition, the final refined position of the cobalt ion in model 1 is in excellent agreement with that predicted from both the native anomalous difference Patterson function and the cobalt − calcium difference Fourier map (Figure 1). In the case of model 2, the cobalt − calcium difference Fourier map does not show any of the strong negative or positive peaks found in the case of model 1, as would be expected from the strong similarity between the SNase−Ca^{2+}−pdTp and Co2 metal-binding sites (map not shown).

Comparison of Overall/Backbone Structures. The overall folds of the two cobalt complex structures are identical to that of the SNase−Ca^{2+}−pdTp structure. Small differences are seen between the three structures in the flexible Ω-loop portion of the protein, comprising residues 42−54. This region does not appear to be well-ordered in any SNase structure determined to date, and so these differences are not surprising [e.g., see Keefe *et al.* (1994)]. Least-squares superposition was used to position either the entire polypeptide chain or residues 7−41 and 54−141 of the two Co^{2+}-complex structures upon the corresponding residues of the Ca^{2+}-complex structure and upon each other; the resulting rms Cα−Cα distances are shown in Table 2. These Cα−Cα distances are of the same general magnitude as the estimated levels of coordinate error, confirming that the backbones of these three protein structures are very similar. Examination of difference distance matrix plots (Kundrot &

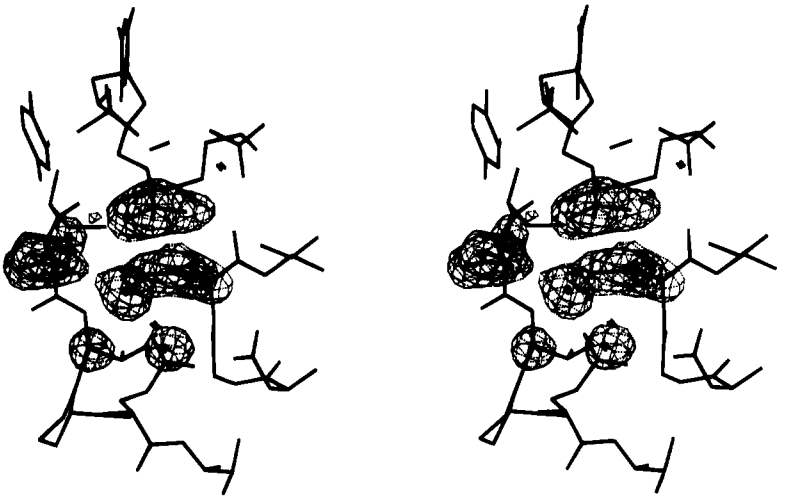

FIGURE 3: Stereoview of an omit electron density map showing the active site of the Co2 structure, calculated with $F_{obs} - F_{calc}$ coefficients like that shown in Figure 2. The contour level is 3σ.

Table 2: RMS Cα−Cα Distances after Least-Squares Superposition (Å)[a]

	SNase−Ca^{2+}−dTp	Co1	Co2	apo-SNase
SNase−Ca^{2+}−pdTp		0.20	0.18	0.41
Co1	*0.27*		0.17	0.41
Co2	*0.26*	*0.30*		0.42
Apo-SNase	*0.70*	*0.74*	*0.70*	

[a] Distances above the diagonal represent rms Cα−Cα distances after least-squares superposition of residues 7−41 and 54−141; the italicized distances below the diagonal represent rms distances after superposition of residues 7−141, inclusive.

Table 3: Distance (Å) from Metal to Ligand in Ternary SNase−Metal-pdTp Complexes

ligand	SNase−Ca^{2+}−pdTp	Co1	Co2
Asp-21 OD1	2.39		2.66
Asp-40 OD1	2.31	2.51	2.58
Thr-41 carbonyl oxygen	2.67		2.96
pdTp O15	2.74	2.32	3.17
water 1[a]	1[a]	2.53	2.43
water 2	2.24	2.51	
water 3	2.45		2.82
water bridging Co^{2+} and Asp-21		1.94	

[a] Convention for numbering aquo ligands: water 1 is equatorial, opposite Asp-40, and adjacent to Asp-21; water 2 is equatorial, opposite Asp-21, and adjacent to Asp-40; water 3 is polar, opposite 5′-phosphate oxygen from pdTp.

Richards, 1987; Loll & Lattman, 1990) showed little evidence for systematic differences between the three structures except for the Ω-loop regions and the region around residue 70 of Co1, which differs slightly from the corresponding regions in the calcium and Co2 structures (plots not shown).

Comparison of the Active Site Regions. The calcium ion in the SNase−Ca^{2+}−pdTp structure is found in an octahedral complex, heptacoordinated by the side chains of Asp-21 and Asp-40, the carbonyl oxygen of Thr-41, a 5′-phosphate oxygen of pdTp, and three waters (see Figure 4a). In addition, the putative general base Glu-43 is tethered to the metal via a bridging inner sphere water. Replacement of the calcium ion with cobalt gives rise to significant perturbations of the active site regions of both cobalt structures, but the changes produced by the metal substitution are different in Co1 and Co2.

In Co1 the cobalt ion is observed to bind 1.94 Å from the calcium binding site (Figure 4b). The coordination of the metal is still octahedral, but only five ligands are seen. The metal still binds Asp-40 and the 5′-phosphate of pdTp, but it does not bind directly to Asp-21; rather, a water molecule has been inserted between the metal and Asp-21. This water molecule occupies approximately the same position as would the calcium ion and bridges the side chain carboxylate of Asp-21 and the cobalt. Two other water molecules contribute equatorial ligands, bringing the total to five. Very weak electron density for a sixth, polar, ligand, presumably a water molecule, can be discerned beneath the metal but was judged too weak to justify inclusion of the water in the model. The pdTp molecule occupies essentially the same position it does in the calcium complex. The water molecule positioned between Asp-21 and the Co^{2+} ion has a metal−oxygen distance of 1.94 Å, near the minimum allowable distance for a cobalt(II)−carboxylate interaction (Carrell *et al.*, 1988). The other four ligands, however, are found at distances ranging from 2.3 to 2.5 Å (Table 3), distances that are longer than optimal for cobalt(II). The refined temperature factor of the cobalt ion is quite high (73 $Å^2$). Together with the long coordination distances, this may reflect high mobility of the metal ion within its coordination "cage". The insertion of a water molecule between the metal and Asp-21 causes the metal to be pushed outward, toward the exterior of the protein. Because the metal retains Asp-40 and the 5′-phosphate as ligands, this outward motion is best described as a rigid body rotation of the metal and its ligands about a distant point lying on a line bisecting the angle formed by Asp-40, the Co^{2+} ion, and the 5′-phosphate. As a result of the metal complex swinging outward and upward, Glu-43 cannot hydrogen bond to an equatorial water ligand, as it does in the calcium structure; rather, in this structure it is found to move downward, to a position under the metal, and to interact with the side chain of the symmetry-related Lys-70*.[2] Lys-70* is also seen to interact with Glu-43 in the calcium complex structure. However, in the Co1 structure Lys-70* forms an additional salt bridge with Asp-21. Hence, in Co1 Lys-70* penetrates more deeply into the active site

[2] The use of an asterisk to mark a specific residue is taken to denote that this residue belongs to a symmetry-related molecule in the crystal lattice.

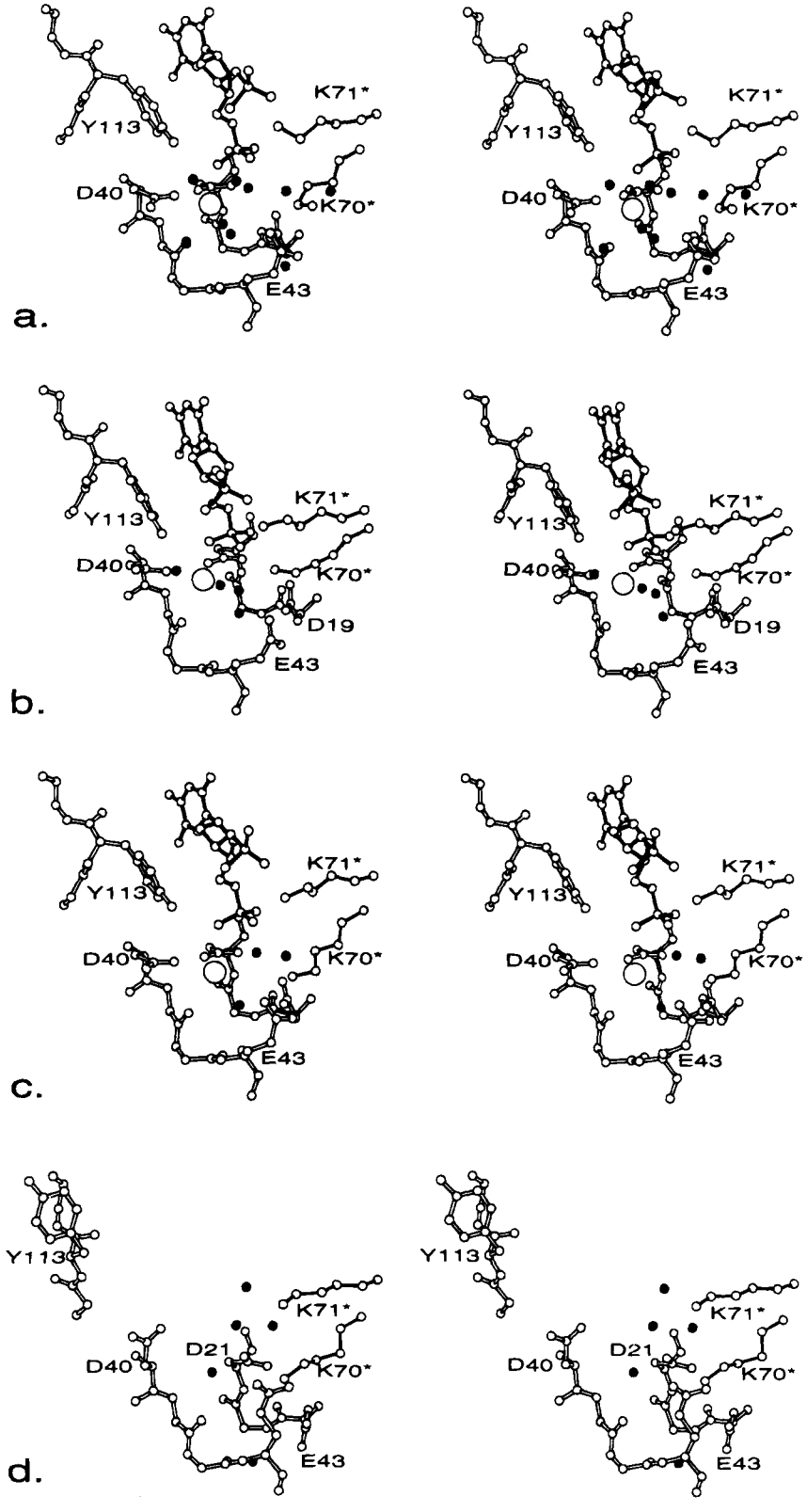

FIGURE 4: Stereoviews of the active sites of different SNase structures. The pdTp molecule is shown at center top with dark bonds. The symmetry-related lysine side chains Lys-70* and Lys-71* are seen at right, also with dark bonds. Metal ions appear as large spheres at the center of the figure; water molecules are shown as smaller black spheres. In the interest of clarity, not all side chains are labeled in all panels. (a) The SNase−Ca^{2+}−pdTp complex. All ordered water molecules found in the active site are shown. *(b)* The active site of the Co1 structure. Only selected water molecules are shown for clarity. Note the presence of a water molecule interposed between the metal ion and the side chain of Asp-21; note also the close approach of Lys-70* to Asp-21. (c) The active site of the Co2 structure. The metal ion now occupies essentially the same position as the calcium ion in panel a, above. Only the inner sphere water ligands and one second sphere water are shown for clarity; the other active site water molecules are essentially the same as shown in the calcium complex, above. Note the absence of the equatorial water ligand opposite Asp-21 and adjacent to Asp-40; this water *is* present in the calcium complex structure seen in panel a. (d) The active site of apo-SNase. Note the tight interaction between Lys-70* and Asp-21.

than in the calcium structure. Metal-to-ligand distances in the Co1 active site are shown in Table 3.

The Co2 structure resembles that of the calcium complex much more than does the Co1 structure. In Co2 the cobalt ion is also displaced relative to the position of the calcium, but the magnitude of the displacement is only 0.36 Å, with the direction of the displacement being again toward the exterior of the protein (Figure 4c). The cobalt ion is octahedrally coordinated by the same ligands as the calcium ion except for one equatorial inner sphere water, which is not evidenced in the Co2 structure. The corresponding water molecule in the calcium complex structure bridges Glu-43 to the metal. As a result of the loss of the bridging water, the side chain of Glu-43 moves 0.3 Å closer to the metal. The resulting 4.4 Å metal-to-oxygen distance is, however, still too large for direct coordination of the metal by Glu-43; small molecule crystallographic studies [e.g., see Poojary and Manohar (1986) and Clark and Orbell (1978)] have shown that the typical Co^{2+}−oxygen coordination bond length is approximately 2.0−2.2 Å. In the Co2 metal ion binding pocket there are no potential liganding partners within that distance that might replace the missing equatorial water. Hence, this liganding position of the metal appears to be empty in the Co2 structure. Obviously, the X-ray experiment yields a static, time-averaged picture of the cobalt environment, and so the apparent absence of this ligand may represent a shortened residence time of the water molecule in the liganding position, a smearing of the water over a large number of positions, or a genuine absence of any specifically bound water in this position. Apart from the absence of this aquo ligand, the small displacement of the metal ion, and the small movement of the Glu-43 side chain, the Co2 active site is virtually identical to that of the calcium complex structure. All other active site water molecules are conserved between the Co2 and calcium complex structures, and all the amino acid side chains around the metal adopt the same conformations as their counterparts in the calcium complex. Metal-to-ligand distances for the metal binding pocket of Co2 are presented in Table 3. As is the case in the Co1 structure, the metal−ligand distances are longer than one would predict for cobalt(II) coordination, suggesting that the positions of the ligands are largely determined by the protein, and that the binding of the Co^{2+} ion is not sufficiently strong to distort the protein geometry so as to satisfy the metal's liganding requirements. The refined thermal factor for the metal ion in Co2 is higher than that of the calcium, although not as high as that observed for the metal ion in Co1 (43 $Å^2$ for the cobalt ion in Co2 versus 73 $Å^2$ for the ion in the Co1 structure and 20 $Å^2$ for Ca^{2+} in the calcium complex structure). Since the Co^{2+} ion is binding in a pocket that has been evolutionarily optimized for the larger Ca^{2+} ion, this higher mobility is not surprising.

DISCUSSION

Co1 versus Co2. A striking result to emerge from this analysis is the finding that two enzyme−metal−nucleotide complexes, identical in composition and formed under similar conditions, can adopt two distinctly different geometries around the metal site. We can present several possible explanations for this. First, it is possible that both complexes coexist and what we observe is simply polymorphism. Second, it is possible that the protein originally crystallized as the Co1 structure and subsequently underwent a transition to form Co2. A possible cause for such a transition would be the drop in water concentration in the crystalline mother liquor which occurred during between the collection of data sets 1 and 2. Such a reduction in water activity might give rise to a small rearrangement in protein packing which might cause the rearrangement of the Co1 structure to the calcium-complex-like structure of Co2, with a concomitant shrinkage in the unit cell parameters. Our data do not allow us to distinguish between these two possibilities; however, given that we have not previously observed crystal polymorphism with any SNase mutant or complex (P.J.L., S.Q., and E.E.L., unpublished) and given the ease with which subtle changes in protein crystal packing can be elicited by small changes in solvent conditions (Moras *et al.*, 1980; Stehle & Schultz, 1992), we suspect the latter is the more likely explanation. A third possibility that must be considered is that during the 9 months that elapsed between the collection of data sets 1 and 2 the metal ion underwent an oxidation to the cobalt(III) form. The rate of ligand exchange would be expected to be very different between a cobaltous and a cobaltic complex, and it is possible that this effect might favor binding of one oxidation state in one site and the other in a second site. Neither Co^{2+} nor Co^{3+} activate the enzyme for nucleic acid hydrolysis, and so structural inferences drawn from these structures about why cobalt ions do not support catalysis should be valid in either case.

The Role of Symmetry-Related Lysines. In the crystal, the side chains of Lys-70* and Lys-71* from a symmetry-related molecule protrude into the active site of the enzyme[3] and interact with the pdTp molecule and active site residues. In the SNase−Ca^{2+}−pdTp, Co1, and Co2 structures, Lys-71* is positioned identically, midway between the 3′- and 5′-phosphates of the inhibitor. However, the role of Lys-70* appears to differ between the various structures. In the calcium complex, Lys-70* forms a salt bridge with Glu-43, and a similar salt bridge is observed in the Co2 structure. On the other hand, while Lys-70* indeed forms a salt bridge with Glu-43 in the Co1 structure, it also forms a salt bridge with Asp-21. This Lys-70*−Asp-21 interaction would not be possible in the calcium complex or its isostere the Co2 complex; in these structures, the equatorial aquo ligand of the metal that is opposite Asp-40 and adjacent to Asp-21 blocks the access of Lys-70* to Asp-21.

The Lys-70*−Asp-21 salt bridge is also seen in apo-SNase (Hynes & Fox, 1991; PDB entry 1STN). The active site of Co1 appears to be a hybrid structure, exhibiting characteristics of both the SNase−Ca^{2+}−pdTp complex and the apoenzyme. Like the calcium complex, the Co1 structure features a bound molecule of pdTp, rearrangements of Tyr-113 and Asp-40 associated with binding pdTp, and an adjustment of the positions of Asp-19 and Asp-21 in response to metal binding. However, unlike the calcium complex and like the apoenzyme, the Co1 structure preserves the interaction between Asp-21 and Lys-70*, even at the expense of significantly distorting the protein backbone around Lys-70*; as a result, the normal metal binding site is blocked and the cobalt ion must occupy a position nearly 2 Å away. One possible interpretation of this observation is that the Lys-

[3] If one is examining the active site of an enzyme molecule located at the general position x, y, z, then the side chains of Lys-70* and Lys-71* are derived from an enzyme molecule related to the first by the transformation $1 - y, x, z + 1/4$.

70*−Asp-21 interaction that occurs during crystallization is a relatively stable one, and only a metal with a high affinity, such as Ca^{2+}, can dislodge Lys-70* from Asp-21 and enter the metal site. A smaller ion with a lower affinity, such as Co^{2+}, may be unable to fully disrupt this strong interaction. Failing to enter the normal metal site, it lodges in a nearby subsite, retaining some of the normal ligands of the metal. This Co1 cobalt ion site may then represent a vestibular site the metal ion normally passes through when adding itself to the binary SNase−pdTp complex. During crystallization of the calcium complex, Ca^{2+} would be expected to proceed smoothly from this intermediate site directly to its normal binding site. However, in the case of cobalt(II), the ion does not bind sufficiently strongly to the normal metal site to displace Lys-70* and hence remains stranded in the vestibular site. After a prolonged period and shifts in the water content of the crystal mother liquor, subtle changes in protein crystal packing may occur which allow the Lys-70*−Asp-21 salt bridge to be broken, followed by a relaxation of the structure into a form very close to that adopted in the presence of Ca^{2+} and pdTp.

The existence of intermolecular contacts which extend into the active site complicates the interpretation of these structures and raises the question of which is more relevant to the SNase−Co^{2+}−substrate complex in solution. Since either mode of Co^{2+} binding will block the calcium site, both structures are consistent with the competitive nature of Co^{2+} inhibition. The Co1 structure seems unlikely to occur in solution, since in it the metal position appears to be determined by the Asp-21−Lys-70* salt bridge. However, while Co1 is unlikely to represent a solution structure, it does provide the information that under conditions where Ca^{2+} is able to elicit the side chain rearrangements necessary for it to enter the metal site, Co^{2+} is not, suggesting at least indirectly that the interactions of Co^{2+} with the metal site are not strongly favorable. On the other hand, the Co2 structure is extremely similar to the SNase−Ca^{2+}−pdTp complex, and we believe it offers information that is directly relevant to questions about why Co^{2+} fails to activate the enzyme and about what role may be played by the Ca^{2+} ion during catalysis. This belief is based on several, we think reasonable, assumptions: (1) The Co^{2+} site occupied in the structure is the same as that in solution. Since the Co^{2+} binds in the Ca^{2+} site, this is consistent with the observed competitive inhibition. (2) The Co^{2+} binding is not distorted by the presence of crystal contacts involving Lys-70* and Lys-71*. In the Co2 and calcium structures, the metal position does not appear to be directly affected by these contacts; the closest approach of the Lys-70* side chain to the metal is almost 5 Å, placing it well outside the second coordination sphere. In contrast, the position of the 3′-phosphate group of the pdTp in both the Co2 and calcium complex crystal structures is probably perturbed by its interaction with the side chain of Lys-71*, an important caveat that must be borne in mind when extrapolating from the crystal structure of any SNase complex to a catalytically relevant structure. Nonetheless, as indicated by NMR docking experiments (Weber *et al.*, 1993), the combination of X-ray and solution results can be used to overcome these problems and provide structural information of mechanistic relevance (Weber *et al.*, 1992).

Implications for Catalysis. It has been suggested that a primary role of the calcium ion during catalysis is the electrostatic stabilization of the presumptive trigonal bipyramidal transition state (Cotton *et al.*, 1979). Our Co2 structure argues that this is not the only role played by the calcium ion, since the Co^{2+} ion occupies essentially the same position as does the calcium and carries the same charge. A transition state structure has been proposed (Weber *et al.*, 1992) that appears to place structural, as well as electrostatic, requirements upon the metal ion; arguably, if the active site is extremely finely tuned to accept this transition state, the small difference in positions of the Co^{2+} and Ca^{2+} ions may suffice to prevent catalysis in the presence of cobalt ion. However, the active site of SNase has been shown to be highly plastic: Mutant forms of the enzyme exhibiting gross distortions in the metal binding pocket still bind calcium and nucleotide (Keefe *et al.*, 1994; Libson *et al.*, 1994) and, in at least one case (the insertion mutant 36L37), exhibit enzymatic activity that is substantially greater than that shown by the wild-type−Co^{2+} complex (Sondek & Shortle, 1992). Hence it appears unlikely that a perturbation as small as a translation of less than 0.4 Å in the metal position should be sufficient to abolish activity.

A catalytic model that has enjoyed long acceptance stipulates that Glu-43 participates in catalysis as a general base, activating either an inner sphere or a second sphere water for attack on the phosphodiester bond. Early structural work led to the identification of a particular second-sphere water as a candidate for the attacking nucleophile, since it was hydrogen bonded to both the carboxylate of Glu-43 and a 5′-phosphate oxygen of pdTp (Cotton *et al.*, 1979). However, our Co2 structure shows this second sphere water is found in the presence of Co^{2+} as well as Ca^{2+} and plays the same structural role in both cases, bridging Glu-43 to the 5′-phosphate of the inhibitor. Given the very low activity of the SNase−Co^{2+} complex, this argues that this second sphere water is not the attacking nucleophile. More recently, workers have put forward a different water molecule as the attacking nucleophile, while retaining the notion of general base catalysis by Glu-43 (Weber *et al.*, 1992). Here, the candidate is the inner sphere water molecule found in an equatorial position adjacent to Asp-40. The Co2 crystal structure is consistent with this hypothesis; we see no evidence for this water molecule in our highly refined Co2 crystal structure. One can therefore propose that the observed lack of SNase activation in the presence of Co^{2+} ion is due to cobalt's inability to bind and position this particular water molecule in such a way as to support catalysis. The lack of a water ligand in this position is somewhat surprising, given cobalt(II)'s predilection for octahedral coordination (Glusker, 1991). It can perhaps be explained by the fact that the Co^{2+} ion is occupying a pocket that is too large for it. Since the ligand positions appear to be dictated by the protein structure, rather than the metal, the ligands cannot collapse inward to optimize the cobalt−ligand distances. Due to the smaller ionic radius of cobalt compared to calcium, the ligands would have to move roughly 0.5 Å in order to tightly ligate the cobalt ion. This would lead to a large scale perturbation of backbone atoms in the region, exacting a high energy cost. Hence the cobalt ion may sample a larger amount of coordination space within the metal binding pocket than does the calcium. The mobility of the metal and the unusually long bond distances would then combine to make positioning of this seventh ligand unfavorable.

The previous argument demonstrates that the Co2 structure offers support to a model involving general base catalysis by Glu-43, wherein an inner sphere water adjacent to Asp-40 is activated for attack on the phosphodiester bond. However, recent results challenge the importance of general base catalysis in the SNase mechanism. Judice *et al.* (1993) have generated catalytically active enzyme containing the unnatural amino acid *S*-4-nitro-2-aminobutyric acid at position 43. While this amino acid is isosteric with glutamate and can function as a bidentate hydrogen bond acceptor, its basicity is very low. This suggests that Glu-43 need not function as a base during the SNase catalytic cycle. In addition, Hale *et al.* (1993) have used pH-rate profile studies of SNase to demonstrate that k_{cat} is dependent upon pH, even at pH values well above the pK_a of glutamate; these results are not consistent with general base catalysis mediated by Glu-43. The loss of catalytic activity in Glu-43 mutants may therefore be due to structural changes in the flexible Ω-loop which adjoins the active site (Loll & Lattman, 1990).

If the attacking water nucleophile is not activated by Glu-43, it may instead be activated by the calcium ion. It has been shown that metal-bound water molecules can display dramatic reductions in pK_as, thereby providing a source of potent nucleophiles at neutral pH (Fersht, 1977; Buckingham & Engelhardt, 1975; Brown *et al.*, 1985). If the Ca^{2+} is the base which activates the attacking water, then this water must be directly coordinated to the metal in an inner sphere position. Using the same arguments presented by Weber *et al.* (1992) in support of their general base mechanism, we can identify the same water molecule as the most likely candidate for a metal-activated nucleophile, to wit, the equatorial inner sphere water adjacent to Asp-40. We propose, then, a tentative mechanism which is essentially identical to that of Weber *et al.* (1992), save for the fact that the calcium ion, and not Glu-43, is responsible for the activation of the attacking nucleophile. This is fully consistent with our Co2 structure, since the principle difference between the Co2 structure and the SNase–Ca^{2+}–pdTp structure is the absence of this inner sphere water in the cobalt structure. It also provides a possible explanation for the inability of Co^{2+} to activate SNase; since the cobalt ion is only loosely held in the too-large calcium binding pocket, it may be unable to tightly bind and polarize a water molecule at the appropriate coordination position. The lack of a reasonable concentration of this metal-coordinated hydroxide ion would mean that a properly positioned and reactive nucleophile is not available to attack the substrate, and hence the enzyme would not be active in the presence of Co^{2+}.

Conclusions. The X-ray crystal structures of two SNase–Co^{2+}–pdTp complexes reveal that two complexes of identical composition can adopt distinctly different conformations in their metal-binding regions, further demonstrating the plasticity of the SNase active site. Both complex structures are shown to be affected by a crystallographic artifact which places lysine side chains from a symmetry-related molecule in the crystal lattice in the enzyme's active site. However, interpretation of these structures in the light of results from solution experiments and docking studies suggests that, in addition to helping to neutralize the charge on the nucleic acid substrate, the role of the calcium ion in catalysis is to activate a specific inner sphere water for nucleophilic attack. One of the cobalt complex structures is very similar to that of the corresponding calcium complex, except that this inner sphere water is completely absent from the cobalt complex. Hence, the failure of cobalt(II) to activate SNase can perhaps be traced to the inability of a Co^{2+} ion occupying the enzyme's metal site to tightly bind and polarize this inner sphere water.

ACKNOWLEDGMENT

We thank Alan Meeker and David Shortle for their kind gift of purified SNase and Al Mildvan and Marvin Makinen for useful discussions. Diffraction data were collected at the X-ray facility of the Department of Biochemistry and Molecular Biology at the University of Chicago.

REFERENCES

Arnone, A., Bier, C. J., Cotton, F. A., Day, V. W., Hazen, E. E., Richardson, D. C., Richardson, J. S., & Yonath, A. (1971) *J. Biol. Chem. 246*, 2302–2316.

Brown, R. S., Dewan, J. C., & Klug A. (1985) *Biochemistry 24*, 4785–4801.

Brünger, A. T. (1992) *X-PLOR Manual, Version 3.1*, Yale University Press, New Haven, CT.

Buckingham, D. A., & Engelhardt, L. M. (1975) *J. Am. Chem. Soc. 97*, 5915–5917.

Carrell, C. J., Carrell, H. L., Erlebacher, J., & Glusker, J. P. (1988) *J. Am. Chem. Soc. 110*, 8651–8656.

Clark, G. R., & Orbell, J. D. (1978) *Acta Crystallogr. B34*, 1815–1822.

Cotton, F. A., Hazen, E. E., Jr., & Legg, M. J. (1979) *Proc. Natl. Acad. Sci. U.S.A. 76*, 2551–2555.

Evans, P. A., Kautz, R. A., Fox, R. O., & Dobson, C. M. (1989) *Biochemistry 28*, 362–370.

Fersht, A. R. (1977) *Enzyme Structure and Mechanism*, pp 49–51, W. H. Freeman, San Francisco.

Glusker, J. P. (1991) *Adv. Protein Chem. 42*, 1–76.

Hale, S. P., Poole, L. B., & Gerlt, J. A. (1993) *Biochemistry 32*, 7479–7487.

Hibler, D. W., Stolowich, N. J., Reynolds, M. A., Gerlt, J. A., Wilde, J. A., & Bolton, P. H. (1987) *Biochemistry 26*, 6278–6286.

Hynes, T. R., & Fox, R. O. (1991) *Proteins 10*, 92–105.

Judice, J. K., Gamble, T. R., Murphy, E. C., de Vos, A. M., & Schultz, P. G. (1993) *Science 261*, 1578–1581.

Kabsch, W. (1988) *J. Appl. Crystallogr. 21*, 916–924.

Keefe, L. J., Quirk, S., Gittis, A., Sondek, J., & Lattman, E. E. (1994) *Protein Sci. 3*, 391–401.

Kundrot, C. E., & Richards, F. M. (1987) *J. Mol. Biol. 193*, 157–170.

Libson, A. M., Gittis, A. G., & Lattman, E. E. (1994) *Biochemistry 33*, 8007–8016.

Loh, S. N., & Markley, J. L. (1994) *Biochemistry 33*, 1029–1036.

Loll, P. J., & Lattman, E. E. (1989) *Proteins 5*, 183–201.

Loll, P. J., & Lattman, E. E. (1990) *Biochemistry 29*, 6886–6873.

Mehdi, S., & Gerlt, J. A. (1982) *J. Am. Chem. Soc. 104*, 3223–3225.

Messerschmidt, A., & Pflugrath, J. W. (1987) *J. Appl. Crystallogr. 20*, 306–315.

Mildvan, A. S., & Serpersu, E. H. (1989) in *Metals Ions in Biological Systems* (Sigel, H., & Sigel, A., Eds.) pp 309–334, Marcel Dekker, Inc., New York.

Moras, D., Comarmond, M. B., Fischer, J., Weiss, R., Thierry, J. C., Ebel, J. P., & Giegé, R. (1980) *Nature 288*, 669–674.

Poojary, M. D., & Manohar, H. (1986) *J. Chem. Soc., Dalton Trans.*, 309–312.

Radzicka, A., & Wolfenden, R. (1995) *Science 267*, 90–93.

Serpersu, E. H., Shortle, D., & Mildvan, A. S. (1986) *Biochemistry 25*, 68–77.

Serpersu, E. H., McCracken, J., Peisach, J., & Mildvan, A. S. (1988) *Biochemistry 27*, 8034–8044.

Sondek, J., & Shortle, D. (1990) *Proteins 7*, 299–305.

Sondek, J., & Shortle, D. (1992) *Proteins 13*, 132–140.

Stanczyk, S. M., & Bolton, P. H. (1992) *Biochemistry 31,* 6396−6401.

Stehle, T., & Schulz, G. E. (1992) *Acta Crystallogr. B48,* 546−548.

Steigemann, W. (1974) Ph.D. Thesis, Technical University of Munich.

Torchia, D. A. Sparks, S. W., & Bax, A. (1989) *Biochemistry 28,* 5509−5524.

Tucker, P. W., Hazen, E. E., & Cotton, F. A. (1978) *Mol. Cell. Biochem. 22,* 67−77.

Tucker, P. W., Hazen, E. E., & Cotton, F. A. (1979) *Mol. Cell. Biochem. 23,* 131−141.

Weber, D. J., Mullen, G. P., & Mildvan, A. S. (1991) *Biochemistry 30,* 7425−7437.

Weber, D. J,. Gittis A. G., Mullen, G. P., Abeygunawardana, C., Lattman, E. E., & Mildvan, A. S. (1992) *Proteins 13,* 275−287.

Weber, D. J., Serpersu, E. H., Gittis, A. G., Lattman, E. E., & Mildvan, A. S. (1993) *Proteins 17,* 20−35.

Wilde, J. A., Bolton, P. H., Dell'Acqua, M., Hibler, D. W., Pourmotabbed, T., & Gerlt, J. A. (1988) *Biochemistry 27,* 4127−4132.

BI942527S